ELSEVIER

Remote Sensing of Environment

Quantifying Vegetation Change in Semiarid Environments: Precision and Accuracy of Spectral Mixture Analysis and the Normalized Difference Vegetation Index

Andrew J. Elmore, John F. Mustard,* Sara J. Manning† and David B. Lobell‡*

Because in situ techniques for determining vegetation abundance in semiarid regions are labor intensive, they usually are not feasible for regional analyses. Remotely sensed data provide the large spatial scale necessary, but their precision and accuracy in determining vegetation abundance and its change through time have not been quantitatively determined. In this paper, the precision and accuracy of two techniques, Spectral Mixture Analysis (SMA) and Normalized Difference Vegetation Index (NDVI) applied to Landsat TM data, are assessed quantitatively using high-precision in situ data. In Owens Valley, California we have 6 years of continuous field data (1991–1996) for 33 sites acquired concurrently with six cloudless Landsat TM images. The multitemporal remotely sensed data were coregistered to within 1 pixel, radiometrically intercalibrated using temporally invariant surface features, and geolocated to within 30 m. These procedures facilitated the accurate location of field-monitoring sites within the remotely sensed data. Formal uncertainties in the registration, radiometric alignment, and modeling were determined. Results show that SMA absolute percent live cover (%LC) estimates are accurate to within ±4.0%LC and estimates of change in live cover have a precision of ±3.8%LC. Furthermore, even when applied to areas of low vegetation cover, the SMA approach correctly determined the sense of change (i.e., positive or negative) in 87% of the samples. SMA results are superior to NDVI, which, although correlated with live cover, is not a quantitative measure and showed the correct sense of change in only 67% of the samples.

INTRODUCTION

Regional measurements of semiarid vegetation abundance are of great importance for identifying the effects of climate variability and other natural or anthropogenic effects on the environment (Tueller, 1987; Woodwell et al., 1984). Field measurements of abundance, while of high quality, are limited in scope and scale, which limits the feasibility of making regional assessments of change. Satellite imagery provides the large spatial and temporal scales necessary to address this fundamental perspective. However, there are some basic difficulties in using remotely sensed data to study vegetation change. The first involves extracting vegetation abundance from measures of radiance, which is seldom measured in the field by vegetation specialists. The two leading methods, Vegetation Indices (VIs) and Spectral Mixture Analysis (SMA), attempt to overcome the inherent difficulties in using radiance data to quantify vegetation abundance in comparable units to field measures.

Previous ecological assessments have utilized vegetation indices such as the Normalized Difference Vegetation Index (NDVI) to measure vegetation from satellite data (e.g., Rouse et al., 1973; Jackson, 1983; Purevdorj

*Department of Geological Sciences, Brown University, Providence, RI
†Inyo County Water Department, 163 May Street, Bishop, CA
‡Department of Applied Math, Brown University, Providence, RI

Address correspondence to A. J. Elmore, Department of Geological Sciences, Brown University, Providence, RI 02912, USA. E-mail: Andrew_Elmore@Brown.edu
Received 12 March 1999; revised 21 January 2000.

655 Avenue of the Americas, New York, NY 10010

0034-4257/00/$–see front matter
PII S0034-4257(00)00100-0

et al., 1998). There is evidence, however, that NDVI is affected by soil color and is therefore not always comparable across a heterogeneous scene (e.g., Major et al., 1990; Elvidge and Lyon, 1985; Huete and Tucker, 1991; Huete et al., 1985; Todd and Hoffer, 1998). Soil and vegetation type normalized indices (Huete, 1988) give results very similar to NDVI since they typically are constrained to two reflectance bands (Lyon et al., 1998). Nevertheless, NDVI has shown a reasonable correlation with vegetation abundance and other important ecological parameters, such as leaf area index (LAI) and fraction of photosynthetically active radiation, and thus continues to be a commonly used indicator of vegetation parameters in remotely sensed data.

The relatively new method of Spectral Mixture Analysis (SMA) (e.g., Adams and Adams, 1984; Mustard and Pieters, 1987) is a promising alternative because it is a physically based approach that produces an estimate of fractional cover of green vegetation in remotely sensed data. However, the precision and accuracy of SMA has not been thoroughly tested in the field. Previous studies (Smith et al., 1990a; Sohn and McCoy, 1997) have compared field measurements from a single date with satellite imagery collected from the same area. Their results show correlation between satellite-derived vegetation abundance and field data, but do not place rigorous estimates on the precision and accuracy of the results. SMA has been applied to studies of land cover change (Adams et al., 1995; Roberts et al., 1997). However, these studies do not quantitatively assess the precision and accuracy of this method for measurements of change.

Garcia-Haro et al. (1996) used SMA and NDVI to measure vegetation abundance from laboratory reflectance spectra of controlled mixtures of soil and vegetation. Both NDVI and the SMA vegetation fractions correlated significantly with laboratory measurements of LAI, but they concluded that the derived abundance of vegetation from SMA was less sensitive to soil background than NDVI. Each method's sensitivity to soil reflectance of multiple soil types in natural conditions should be tested. Garcia-Haro et al. (1996) found the accuracy of mixture model vegetation fraction images to be sufficient for many applications with actual satellite data, but they did not use any satellite or field data in their experiments, leaving the problem open to further studies.

A second challenge in measuring vegetation change arises when comparing field point measurements with the large-scale data acquired by remote sensing systems. In many of the studies discussed above, variables other than the capability of the mixture model or NDVI in dealing with complex data sets are cited as the major sources of error. Precise georeferencing and coregistration of images and the accurate identification of field sites in all images are essential components of multitemporal analysis. Coregistration in particular has been shown to be an important contribution to error in vegetation change measurements (Duncan et al., 1993; Townshend, 1992).

In this article we assess quantitatively the ability of NDVI and SMA to extract meaningful vegetation abundance information from Landsat Thematic Mapper (TM) data from semiarid Owens Valley, California. We also discuss the methodologies required to incorporate ground-based measurements with satellite based measurements. For this study, we utilized field data that were carefully measured at specific time periods spanning several years. The linkage of these two multitemporal data sets provides an unique opportunity to analyze SMA- and NDVI-derived estimates of vegetation cover and its change over time. Many researchers have shown or suspected that soil background and/or community type are the dominant source of deviations between field and remote measures of vegetation abundance. With a multitemporal dataset it may be possible to show that despite constant deviations for specific regions through time, annual change in abundance can be a very accurate and precise measurement.

STUDY AREA AND SITE DESCRIPTIONS

Owens Valley is a hydrologically closed basin in Eastern California. The valley extends approximately 120 km from north to south and is bordered on the west by the Sierra Nevada and on the east by the White-Inyo Range (Fig. 1). The Sierra Nevada forms a rain barrier, effectively blocking the valley from most easterly flowing winter storms and keeping median annual precipitation to 13 cm. Each spring and summer, however, abundant runoff from melting Sierra Nevada winter snow flows into the valley and recharges groundwater aquifers. As a result, the groundwater table on the valley floor is typically high (Hollett et al., 1991).

Owens Valley straddles the boundary between the Great Basin and Mojave Deserts. The valley can be divided into alluvial fan, a gently sloping region with deep water tables and dominated by xeric species, and valley floor, a relatively large (61,500 ha), flat, high water table basin dominated by phreatophytes. Although the vegetation has been broadly characterized as Desert Saltbush Scrub (Kuchler, 1988) recent vegetation mapping efforts, described by Inyo County and City of Los Angeles (1990), list several scrub and meadow plant communities as occurring in the valley, as well as a few riparian and marsh communities. Plant community descriptions follow Holland (1986).

A monitoring network of 33 permanent field sites was used in this study. All sites were located in phreatophytic vegetation on the valley floor. The dominant species at the sites included two perennial grasses, saltgrass (*Distichlis spicata*) and alkali sacaton (*Sporobolus airoides*) and three shrub species: Nevada saltbush (*Atriplex lentiformis* ssp. *torreyi*), rabbitbrush (*Chrysothamnus nauseosus*), and greasewood (*Sarcobatus vermiculatus*) (nomenclature follows Hickman, 1993). All dominants begin annual growth in spring and reach peak leaf area by early

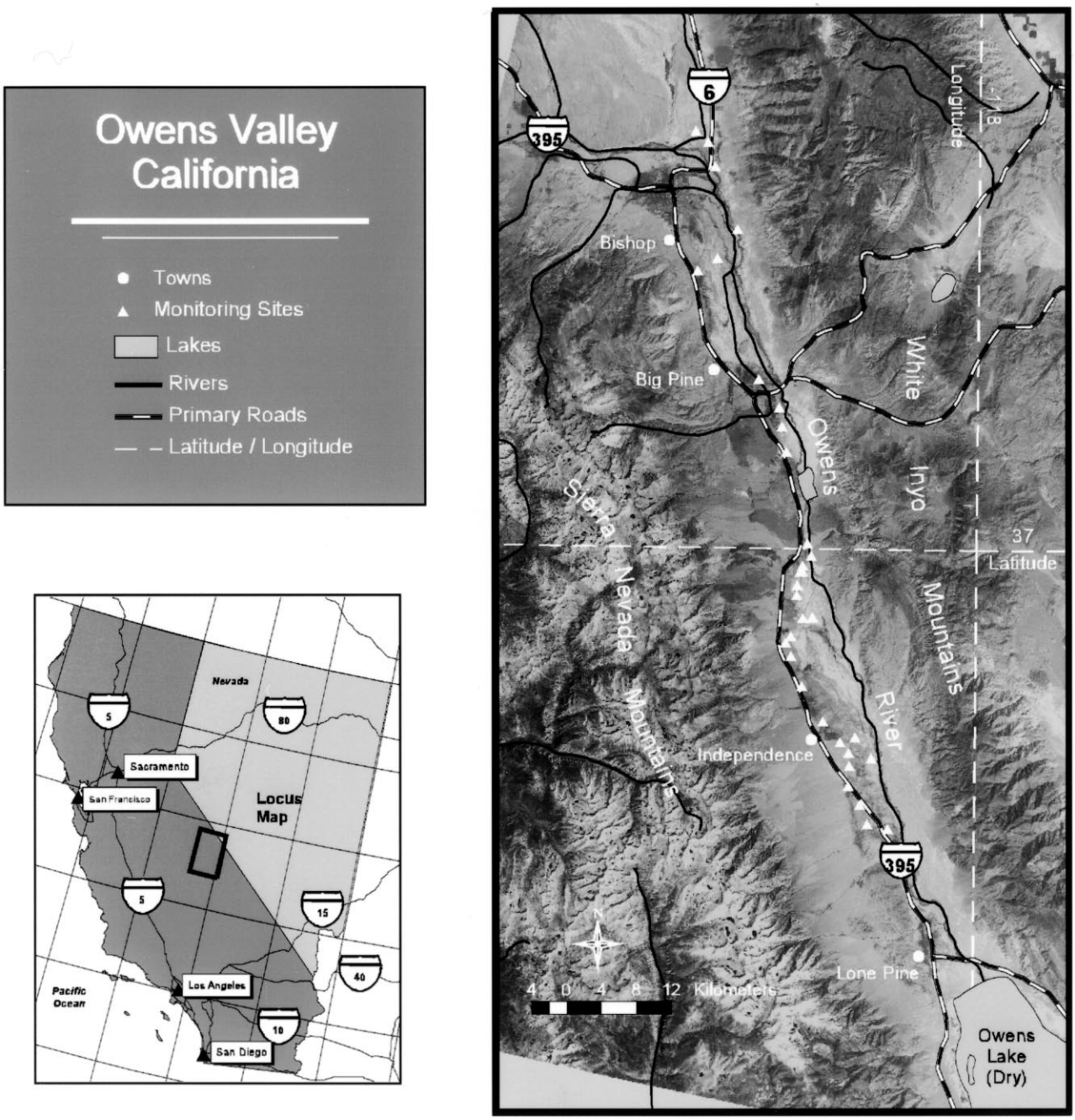

Figure 1. Location of the study area in Owens Valley, California. The distribution of the field sites across the valley floor is indicated by the small triangles.

summer (Sorenson et al., 1991). Despite floristic similarities, there was a wide range in proportions of grasses and shrubs at the sites, and some sites had a high percentage of annual forb species. Average percent live cover (1991–1996) ranged from 5% to nearly 50% (Table 1).

DATA ACQUISITION

Image Data and Preprocessing

Fourteen Landsat Thematic Mapper images were acquired from 1984 to 1997 (Table 2). The Landsat TM sensor has a pixel size of 28.5 m by 28.5 m, with six visible-infrared band passes and one thermal band. Data of Owens Valley were taken from path 41 and shifted 30% from row 34 to row 35. The large Landsat scenes were then reduced to data sets including only the valley itself: 2,425×5,825 pixels each. All of the data sets were selected from relatively cloud-free scenes acquired during late summer or early fall of each year. September was the preferred acquisition month because it ensured that spring ephemeral species were avoided and perennial species had completed their seasonal growth, but had not

Table 1. Permanent Monitoring Sites

Monitoring Site	*Code*	*Dominant 1*	*Dominant 2*	*Grass (%)*[a]	*Shrub (%)*[b]	*Weed (%)*[c]	*Ave % LC*[d]
Bairs-Georges 2	BG2	ATTO	SAVE	<1	100	<1	18.26
Bairs-Georges Control	BGC	ATTO	DISP	3	97	<1	18.16
Big Pine 1	BP1	ATTO	SAVE	2	91	7	17.27
Big Pine 2	BP2	ATTO	CHNA	<1	100	<1	15.67
Big Pine 3	BP3	SAVE	SPAI	8	91	1	9.33
Big Pine 4	BP4	ATTO	SAVE	<1	100	<1	18.11
Bighop Control 1	BC1	ATTO	CHNA	12	88	<1	22.46
Bishop Control 2	BC2	CHNA	DISP	24	75	<1	23.01
Bishop Control 3	BC3	DISP	CHNA	53	37	<1	32.24
Independence Control 1	IC1	ATTO	CHNA	3	97	<1	20.41
Independence Control 2	IC2	SPAI	ATCO	67	32	1	5.59
Independence-Oak 1	IO1	SPAI	ATTO	34	66	<1	24.60
Independence-Oak 2	IO2	ATTO	ATCO	<1	98	2	11.83
Laws 1	L1	SAVE	DISP	1	66	33	5.09
Laws 2	L2	SPAI	SAVE	44	55	<1	10.33
Laws 3	L3	SPAI	ATTO	80	17	2	21.41
Symmes-Shepherd 1	SS1	ATTO	SAVE	<1	100	<1	11.13
Symmes-Shepherd 2	SS2	ATTO	N/A	<1	98	2	13.57
Symmes-Shepherd 3	SS3	ATTO	N/A	<1	92	8	13.07
Symmes-Shepherd 4	SS4	ATTO	N/A	<1	100	<1	15.47
Taboose-Aberdeen 1	TA1	SPAI	ATTO	44	12	44	6.99
Taboose-Aberdeen 2	TA2	ATTO	SAVE	19	81	1	15.77
Taboose-Aberdeen 3	TA3	SPAI	ATTO	27	73	<1	14.57
Taboose-Aberdeen 4	TA4	SPAI	CHNA	64	32	5	12.63
Taboose-Aberdeen 5	TA5	SPAI	SAVE	35	66	<1	4.99
Taboose-Aberdeen 6	TA6	SPAI	CHNA	21	71	8	23.00
Taboose-Aberdeen Control	TAC	ATTO	SPAI	52	29	16	48.95
Thibaut-Sawmill 1	TS1	SPAI	ATTO	39	56	4	26.90
Thibaut-Sawmill 2	TS2	SPAI	ARTR	47	41	10	10.28
Thibaut-Sawmill 3	TS3	SPAI	ATTO	87	13	<1	21.36
Thibaut-Sawmill 4	TS4	SAVE	ATTO	23	77	<1	25.35
Thibaut-Sawmill 6	TS6	SPAI	DISP	60	28	12	19.51
Thibaut-Sawmill Control	TSC	SPAI	CHNA	65	34	<1	8.58

[a] *Sporobolus airoides* (SPAI) and *Distichlis spicata* (DISP).
[b] *Atriplex lentiformis* ssp. *torreyi* (ATTO), *Chrysothamnus nauseosus* (CHNA), *Sarcobutus vermiculatus* (SAVE), and *Atriplex confertifolia* (ATCO).
[c] Species that tend to proliferate in distinct patches. Includes invasive exotics (*Salsola tragus*, *Bassia hyssopifolia*) and native opportunistic species (*Glycyrrhiza lepidota*, *Conyza* sp., *Cleome* sp.).
[d] Average live cover from 1991 through 1996.

begun to senesce in response to freezing temperatures (Sorenson et al., 1991). Spring annuals are highly variable in their phenology and leaf cover, while shrub growth is seasonally more constant and therefore more accurately captures yearly fluctuations in base-level vegetation abundance (MacMahon, 1988). Some scenes were acquired during late August, while the 1985 scene was taken during the first week of October.

Three processing steps were completed on the 14 Landsat TM data sets: (1) coregistration; (2) spectral calibration to temporally invariant surface features; and (3) georeferencing of the dataset. These three steps are critical to the success of all multitemporal remote sensing studies.

1. Using a small number of ground-control points, all images were first aligned with the 1992 image through a simple first-order translation. The aligned images were then partitioned into 32×32 pixel subareas (boxes). Each subarea was then linearly coregistered to the corresponding 1992 box with a determined goodness of fit, r^2, between 0 and 1. All regions with an r^2 greater than 0.9 (~7,000) were then used to perform a weighted second-order geometric coregistration on the entire image. The resulting images were coregistered to well within 1 pixel in most areas and no worse than 2 pixels.
2. It is critical that the radiometric response of a given scene is comparable to that of every other scene. By performing spectral calibration, we assured that spectral differences among the images were due to fundamental change in surface characteristics and not due to changes in the atmosphere, solar elevation and azimuth, and sensor performance. There are several strategies available to achieve a common multitemporal spectral response. We applied the technique of temporally invariant surface features (TISFs) (Hall et al.,

Table 2. Dates of Landsat TM Acquisitions

Year	*Day Month*
1984	1 August
1985	7 October
1986	23 August
1987	29 September
1988	13 September
1989	31 August
1990	3 September
1991	22 September
1992	8 September
1993	26 August
1994	14 September
1995	17 September
1996	3 September
1997	6 September

1991; Schott et al., 1988). TISFs are regions of a scene that are assumed not to change spectrally over the sequence of scenes to be corrected. The method is based on two fundamental assumptions: (1) the radiometric response of the instrument is linear, and (2) all variations due to environmental variables can be accommodated by a linear slope and intercept correction. Four TISF locations were selected. Lava flows with little to no vegetation were chosen as a dark invariant feature. Small, isolated playas on the valley floor were chosen for a bright invariant feature. Two sites of intermediate albedo were chosen from alluvial fans on the eastern side of the valley. Although these two fan sites had a small component of vegetation (<3%), the surfaces were in an area of very little rainfall and were composed of drought-resistant species. Thus the surfaces were expected to change very little over the 14 years of this study. In multitemporal, multiband scatter plots, these four TISFs always fell on a straight line, supporting assumptions of no change at all of the sites. Each band from each image was regressed against the corresponding band from the 1992 image, a line was fit to the points, and all images were then adjusted to have the same spectral response as the 1992 data set. The 1992 data set was used as a reference for this procedure because it was cloudless and temporally near the middle of the total data set.

3. An accurate georeferencing of the dataset was performed by recording the latitude and longitude of 18 different locations with a Global Positioning System (GPS) (Garmin 12XL) spanning Owens Valley and neighboring Fish Lake and Eureka valleys. In general, road intersections were used as GPS points since it was possible to locate them in the image. These GPS points were not differentially corrected, but measured multiple times and averaged for a spatial accuracy within 15 m. In addition to these data points, several tie-points were found near the edges of the image using 7.5-inch USGS maps of area. Finally, 15 more tie-points were identified by comparing the Landsat database with previously georeferenced GIS layers from the Inyo County Water Department GIS database. A combined set of 39 tie-points were used to warp the dataset to a UTM grid (North American 1927 datum) using a third-order polynomial. A set of seven GPS locations and five test points selected from USGS maps were held in reserve to test the georeferencing. Comparisons of these points against common points in the images showed that georeferencing was accurate to within 2 pixels (60 m) throughout the scene, but much of the valley was within 1 pixel (30 m).

Field Data

The 33 permanent monitoring sites were fully implemented by 1990. From 1991 through 1996, water table depth and soil water content were recorded monthly at these sites, and vegetation conditions were measured during the last two weeks of June (mid growing season) and the last two weeks of August (late growing season). Vegetation was measured along a permanently marked 100-m transect using a large point frame (Sorenson et al., 1991). A 100-m tape was stretched between the two transect end posts, and the point frame was positioned along the tape beginning at the zero post. Pins were lowered at 30-cm intervals along the entire length of the transect. At each measurement point, the identity of the first species contacted with a pin, total contacts with all species, and ground cover (litter or bare ground) were recorded.

Percent live cover (%LC) at each transect was calculated by dividing the number of pins that contacted live plants by the total number of pins used (334). Because the transect was run only once at each measurement time, the error in the measurement cannot be calculated directly. However, previous trials to assess this error by running six point frame transect replicates at three different sites showed an average error of any one measurement to be ±2.3%LC (e.g., 10.2±2.3%LC or 15.6± 2.3%LC). These uncertainties are due in part to operator error and variations produced by wind movement of vegetation during a measurement.

METHODS

Spectral Mixture Analysis

The materials in a given picture element (pixel) in remotely sensed data are rarely represented by a single physical component. This is particularly true in arid and

semiarid regions where the distribution of soil and vegetation is highly variable. SMA is based on the concept that the relative proportion of a few spectrally distinct components is what dominates the variance across a given remotely sensed scene. The concept of the mixed pixel has been recognized for many years (Horowitz et al., 1975; Graetz and Gentle, 1982; Pech et al., 1986; Singer and McCord, 1979; Adams and Adams, 1984), and the development of an end-to-end understanding and model has led to quantitative applications (e.g., Mustard and Pieters, 1987; Adams and Adams, 1984; Adams et al., 1986; Adams et al., 1993; Gillespie et al., 1990). SMA has been used to measure %LC of vegetation in several studies of semiarid regions with mixed results (e.g., Smith et al., 1990a; Sohn and McCoy, 1997).

In linear SMA, the spectral properties of a pixel are modeled as a linear combination of endmember spectra weighted by the percent ground coverage of each endmember. Endmembers are fundamental physical components of the scene that themselves are not mixtures of other components. The assumption of a linear model requires that components be arranged in spatially separate areas of the pixel (Singer and McCord, 1979). This configuration reduces the number of multiple reflections, which are more common when mixtures of endmembers are on the scale of the wavelength of electromagnetic radiation detected. Most arrangements of physical materials will produce a nonlinear component (Johnson et al., 1983; Mustard and Pieters, 1989). Nonlinear mixing models have been used successfully with a variety of vegetation types (Borel and Gerstl, 1994; Ray and Murray, 1996). However, the linear approach used here has been shown in many applications to have sufficient accuracy to map vegetation abundance in remotely sensed data (e.g., Adams et al., 1993; Pech et al., 1986; Roberts et al., 1993; Smith et al., 1990a; Smith et al., 1990b).

Endmember spectra selected from the image were used in the following equations. These equations were solved for every pixel in all 14 images [see Eq. (1), Eq. (2), and Eq. (3)]:

$$DN_b = \sum_{i=1}^{N} F_i DN_{i,b} + E_b \quad (1)$$

$$\sum_{i=1}^{N} F_i = 1 \quad (2)$$

$$\text{RMSE} = \sqrt{\sum_{i=1}^{B} \frac{(E_i)^2}{B}} \quad (3)$$

where DN_b is the intensity of a given pixel in band pass or wavelength b, F_i is the fractional abundance of endmember I, $DN_{i,b}$ is the intensity of image endmember I at wavelength b, N is the number of endmembers, and E_b is the error of the fit for band pass b. Thus, for this analysis with TM data, there will be six equations, one for each spectral band (B=6). Equation (2) constrains the sum of the fractions to equal unity; however, there is no constraint that the fractions must be between 0.0 and 1.0. In a strict sense, fractions outside the range of 0.0–1.0 are physically impossible. However, an additional constraint that fractions fit this range can lead to erroneous results. A properly constructed mixture model should return fractions that sum to 1.0 and lie between 0 and 1.0 without any constraint (e.g., Mustard and Pieters, 1987; Mustard and Pieters, 1989). The unity constraint, however, tends to stabilize solutions. Additionally, allowing individual fractions outside the range 0.0–1.0 provides important information on the validity of endmember selection (see below). Equation (3) is the total root-mean square error (RMSE) where B is the total number of spectral bands.

An important behavior of SMA is its invariance under linear transformations. Linear transformations of a dataset, such as reflectance retrieval, do not change the linear addition of endmembers as long as the same linear transformations are performed on the endmembers before the analysis. This feature makes reflectance retrieval unnecessary when using image endmembers because the exact same results will be achieved regardless of this preprocessing step.

Endmembers

The key to a successful mixture model is the selection of appropriate endmembers. Endmembers must define a coherent set of spectra that are representative of physical components on the surface, but they also must model the spectral variability inherent to the scene. Candidate image endmembers were used in trial runs of the model defined by Eqs. (1), (2), and (3). The validity of the endmembers is assessed by analyzing the fraction and RMSE results. The fractions calculated across the scene should lie between 0 and 1 while the RMSE should be uniform and close to the measurement precision of the data (±1–2 *DN*). Images of the fractions and RMSE will show spatial features where the variability of the scene is not adequately expressed by the linear addition of the candidate endmembers. If this was the case for an important area of the valley floor or bajada in any of the 14 images, new endmembers were selected and the model run again. However, poor model results for surfaces outside the scope of this research (e.g., agricultural fields, high altitude regions) were not considered.

In Owens Valley, vegetation, two soils, and shade (to account for illumination effects) were chosen to represent the spectral variability. When the model was run, these endmembers explained the greatest percentage of the scene variance. Our endmembers (Fig. 2) were taken from the image (image endmembers) as opposed to reference endmembers, which are formed from reflectance measurements usually made in the laboratory (Adams et al., 1993). While reference endmembers would have un-

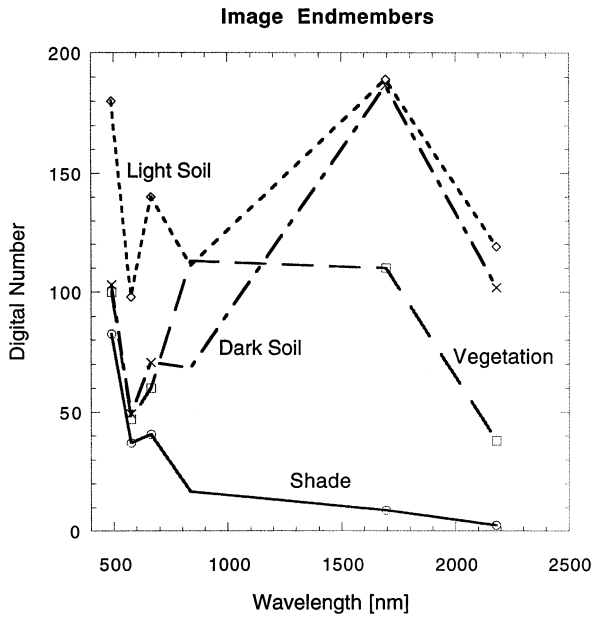

Figure 2. Endmember spectra used in the spectral mixture analysis.

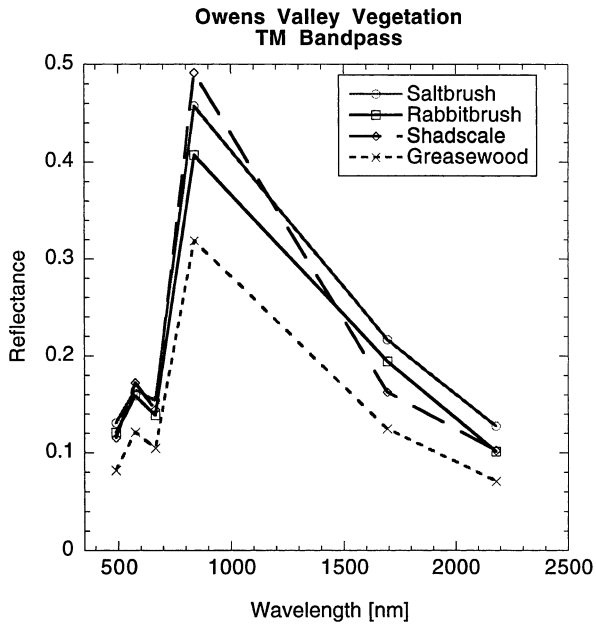

Figure 3. Field spectra (of major species in Owens Valley) converted to TM band pass. Spectra were acquired from dense shrub canopy using an Analytical Spectral Devices portable field spectrometer.

doubtedly represented a more pure endmember spectra and possibly would have given a more accurate absolute abundance, image endmembers simply produce a different scaling and thus can be used for change detection. The decision to use image endmembers also allowed us to bypass reflectance retrieval, which is secondary in importance to intercalibrating for change detection.

The vegetation endmember was selected from a riparian area near the Owens River. While this vegetation is different in species, life form, and leaf morphology and height (i.e., structure) from the typical vegetation in the valley, it was necessary to select an area that approximated 100%LC. At the low spectral resolution of Landsat TM data, most Owens Valley vegetation spectra share a common set of spectral features (Fig. 3).

A light soil endmember was chosen from the bright playas in the southern part of the valley. Soils on the fans and dry parts of the valley floor have a similar high reflectance. A dark soil endmember was chosen from an area in which the soil was high in organic content. Such soils, mollisols (meadow soils) and histosols (marsh soils), are typically found on the western side of the valley where groundwater historically vented in natural springs or seeps. This endmember was chosen from an abandoned agricultural field during a year of low precipitation, and therefore had less than 3% vegetation. Because of the spectral contrast of vegetation, the vegetation fraction images changed very little with changes in soil endmember selection.

The final endmember was shade. While not a physical component of the scene, shade accounts for illumination effects on the sub- and multipixel scale. Shade also accommodates some variations in reflectance due to soil brightness. Because a deep clear lake reflects very little in all TM bandpasses, a large reservoir located near the geographic center of the valley was used. Postprocessing, the vegetation fraction image can be normalized to remove the shade component, such that the remaining endmembers sum to one for each pixel (Adams et al., 1993). This procedure is desirable where shade is negatively correlated with vegetation and soil fraction images. However, in our experience, the shade fraction image was often positively correlated with soil brightness and therefore artificially elevated the live cover in these areas when a scaled vegetation fraction image was calculated.

The single endmember set shown in Fig. 2 is used across the entire suite of 14 images. Along with good spectral calibration, using identical endmembers to analyze multitemporal scenes strengthens the change analysis because it assures that for surfaces that have not changed, any given endmember abundance in one image will be the same endmember abundance in another image. Conversely, changes that we detected should be a direct function of changes in the relative aerial coverage of materials represented by endmembers.

Vegetation Indices

Vegetation indices (VIs) take advantage of vegetation's reflective contrast between the near infrared (NIR) and visible red (VIS) wavelengths. NDVI is given by Eq. (4):

$$\mathrm{NDVI}=\frac{\mathrm{NIR}-\mathrm{VIS}}{\mathrm{NIR}+\mathrm{VIS}} \quad (4)$$

Because NDVI can be affected by soil reflectance (Huete et al., 1985; Elvidge and Lyon, 1985), soil adjusted VIs have been developed to take into account the local soil reflectance. However, these VIs were found to be highly correlated to NDVI such that the choice of one VI over another essentially resulted in a scaling of NDVI (Lyon et al., 1998). For the purpose of this analysis, we compared NDVI to the results of SMA, recognizing that other VIs will exhibit similar relationships.

Before our calculations of NDVI were completed, the same preprocessing steps as with the SMA procedure were performed. As an additional step, field spectra of homogeneous dark, medium, and light soils were used to convert the radiance of the NIR and VIS bands to reflectance using an empirical line method (Roberts et al., 1993). Reflectance retrieval resulted in NDVI values comparable to values found in the literature thus aiding in comparison to other work.

Merging Field and Remotely Sensed Measurements

Differences in spatial and temporal scale between the field and satellite measurements present difficulties in making quantitative comparisons between them. To incorporate the Owens Valley field data, it was necessary to determine which specific pixels in the TM data best matched the ecological unit represented by the 100-m transect. A combination of techniques were used to establish this relationship:

1. The GPS location of the field site coupled with precision georeferencing of the satellite data.
2. GIS layers of roads, canals, and vegetation polygons to identify features in the images.
3. Aerial photos (1:12,000 scale) to link the TM imagery to visible features of the sites.
4. Site visits to record key surface features. A land unit was delineated that apparently encompassed an area of homogeneous land cover with regard to species composition, density, and soil properties as that beneath the 100-m transect line.
5. Correlation and intercept statistics calculated for every pixel in a 9×9 pixel grid centered on the midpoint of the 100-m transect. The statistics were used to confirm that the edge of a road or other man-made object was never included in a pixel being considered for inclusion in the transect unit.

Our goal was to identify the 2×2 pixel sample that best matched the physical location and vegetation unit represented by each 100-m transect. Use of a single pixel to target the transect was rejected due to potential effects of missregistration (discussed later). Likewise any linear grouping of pixels (e.g., 2×1, 3×1, and 3×2) could be affected by registration. In addition, orientation and location of linear groups would be problematic across all of the sites. Thus it was determined that a 2×2 pixel group provided the optimal size to match the satellite to the field measures. Nevertheless, in choosing a 2×2 pixel group to represent the 100-m transect line, we are making the assumption that the heterogeneity within the 60 m by 60 m area is representative of the heterogeneity within the sampled transect. We feel that this is a safe assumption based on air photos and visits to the field sites.

An example of how these different types of data can be used to find the field site in the Landsat dataset is illustrated in Fig. 4. On the right is an airphoto of the IO1 field site. The photo shows how heterogeneity of vegetation cover and roads can make it difficult to find pure pixels of the transect vegetation unit. The image on the left is a 1992 Landsat TM scene, Band 2, for the same area as the photo. Overlaid on this image are GIS layers of roads (white), the 100-m transect line (black), a box outlining the 9×9 sample space (black), and the optimum 2×2 sample box identified to represent the field site (light gray). From this figure it appears that there are several possible positions of the 2×2 sample box that could represent the 100-m transect line. However, using all of the data available, the box presented in Fig. 4 was the best choice.

The percent live cover measured in the field each August was compared with the corresponding measurement made from the Landsat TM data for each site. With 33 field sites and 6 years of observations, this corresponds to 198 measurements. When forming the correlation model, a stratified random subset of the 33 field sites was used. Hypotheses formed and statistical values calculated (such as correlation coefficients) were then tested by applying the same methods to the reserved sites.

Sources of Error

There are three main sources of error that contribute to the uncertainty in the multitemporal estimate of vegetation abundance from SMA and NDVI: (1) multidate registration and field site location, (2) spectral calibration to ground invariant points, and (3) mathematical error in the model. The error due to each of these sources were added in quadrature to calculate the total uncertainty of measurement.

The first and potentially largest source of error is due to missregistration of the multidate scenes and location of the field sites. This source of error is calculated in the same way for both SMA and NDVI. Although coregistration is better than 1 pixel in most areas and never worse than 2 pixels, the degree to which this uncertainty in location affects our results is dependent on the homo-

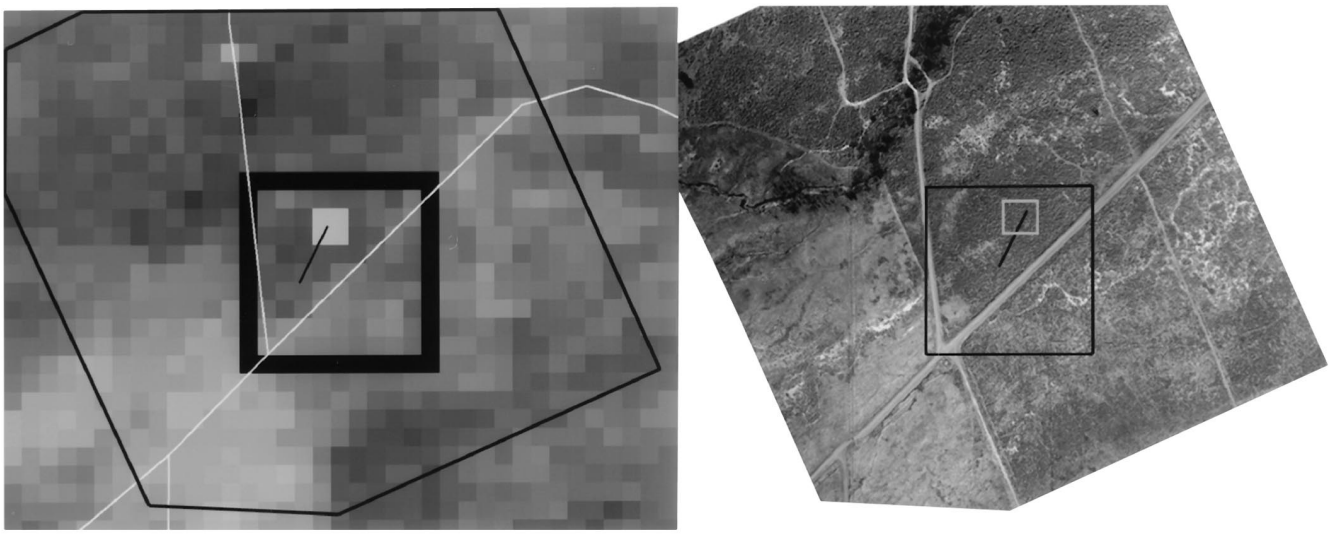

Figure 4. Example of methods used to locate permanent monitoring sites in the TM data. (a) GIS road (gray lines), stream, and aqueduct coverages for site IO1 used to locate each monitoring transect (short black line) in the Landsat TM data. (b) High resolution air photographs of the same site, which were used to refine the location. Boxes represent the same areas as in Fig. 4a.

geneity of the scene at the field site. Therefore, to find standard error for a measurement of vegetation, we calculate the standard deviation of all of the vegetation abundance within 1 pixel of the assumed location of the site. This standard deviation is an estimate of the uncertainty of the measurement within a 70% confidence interval. These errors are site-dependent and range from 0.5% to 4.0% live cover for SMA and 0.010 to 0.035 for NDVI.

The accuracy of the radiometric calibration depends on the spectral invariance of the four surfaces. To assess the effect of noninvariant surfaces on the calculations, we performed a sensitivity analysis on the slope and intercept of the ground invariant point regression. For each dataset, the slope and intercept were each varied ±0.5%, ±1.0%, or held constant. These represented a realistic range of values likely to result from small changes in surface properties. The model was run for each permutation producing a Gaussian distribution of calculated vegetation estimates for SMA and NDVI. The standard deviation of values calculated from these permutations was found to be 1.06% live cover for SMA and 0.01 for NDVI.

The final source of error applies to the calculations of SMA. Error in the SMA estimates of vegetation abundance is a function of the signal-to-noise ratio of the measurements and the spectral contrast of the endmember in question (i.e., vegetation) against the other endmembers in the inversion. This is a formal, model certainty and was determined to be 1.5%.

In addition to the above three sources of error, our selection of endmembers influenced the derived SMA percent live cover. We have taken care to select the most appropriate image endmembers; however, pure pixels at the scale of the TM data are rare and some contamination is likely. As a result, some SMA-calculated %LC measurements are <0 and >100%LC. In Fig. 5, we see that there are five points that fall below zero. These points must be accepted as inaccurate measurements due to impure endmembers.

RESULTS

Vegetation Cover Measurements

The correspondence between %LC determined with SMA and the 33 field sites for 1991 through 1996 (198 measurements) is shown in Fig. 5a, while the correspondence between NDVI and the field measures is shown in Fig. 5b. In Fig. 5a, most of the points corroborate well with the one-to-one line (mean bias is 2.29%LC), demonstrating excellent correlation between SMA and field measures of %LC. Using the Kolmogorov-Smirnov (Davis, 1986) test, it was not possible to reject our hypotheses that the SMA values are a Gaussian distribution about their calculated mean. Therefore, the uncertainty in measuring absolute %LC using SMA was ±4.0%LC (one standard deviation from the mean). The distribution of points about the one-to-one line can be seen more clearly in Fig. 6. This histogram shows the number of points at each distance from the one-to-one line. While the distribution is narrow, the peak falls to the right of the center, indicating that there was an aggregate bias to measurements of absolute %LC.

The relationship between NDVI and %LC is more complicated (Fig. 5b). NDVI is also well correlated with %LC; however, there appears to be slightly more scatter

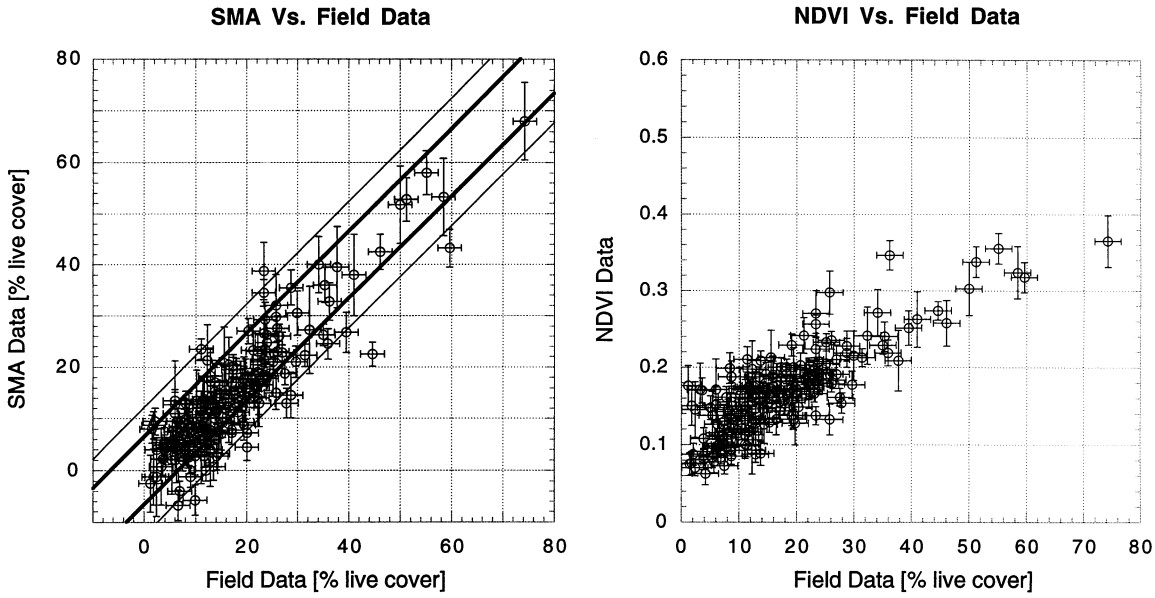

Figure 5. Percent live cover measured in the field (x axis) plotted against (a) SMA results and (b) NDVI. Error bars were determined uniquely for each site as described in the text. For (a) lines at ±4.0 and 8.0%LC are shown about the 1:1 line.

in the relationship. Previous work has shown that both soil brightness and soil spectral effect can influence NDVI (Huete et al., 1985) and that vegetation is overestimated on dark backgrounds relative to bright backgrounds (Elvidge and Lyon, 1985). Also, at lower %LC, NDVI is dominated by the spectral slope of soils from the visible to near-infrared.

Figure 6. A histogram of the absolute %LC estimates from Fig. 5a showing the distribution of the data about the one-to-one line. Note that the distribution peak is off center, indicating a bias.

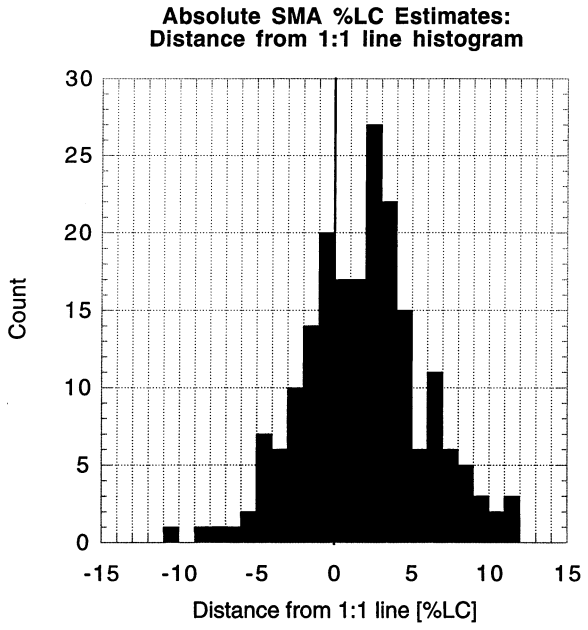

Comparisons of the variation of green vegetation abundance with time determined with the remote measurements (SMA and NDVI) and field measurements provide some insight into the sources of scatter observed in Fig. 5. The IO1 field site (Fig. 7a) is an example where the SMA data closely resembles the field data. In this figure, all field and satellite data are displayed. Seasonal changes in percent live cover are observed in the more frequently measured field data where June measurements typically exhibited higher abundance than August measurements. NDVI results also track the changes somewhat, but do not exhibit the direct correspondence to the field %LC measurements.

Site SS3 demonstrated a different case where SMA results generally track but were apparently offset from the field data, suggesting a bias in the calculations. At this site, the average bias is to underestimate field measures by 12%LC. Sites that exhibit a bias are temporally constant in the magnitude and sign of the bias. This suggests that the physical and ecological properties of the site may contribute in a systematic way to create a bias in the SMA results. Properties such as composition, the dispersion of plants on the site, plant size and vigor, and herbivore impacts are likely to be involved. However, we have not yet identified the controlling factors. Data from sites such as SS3 add to the variance of the data distribution in Fig. 5a because the data plot at a constant distance away from the one-to-one line. As with the IO1 site, NDVI tracked the changes in %LC, but it was more difficult to quantify bias.

Because the bias shown in Fig. 7b is apparently a property of the field site (and not, for example, a prop-

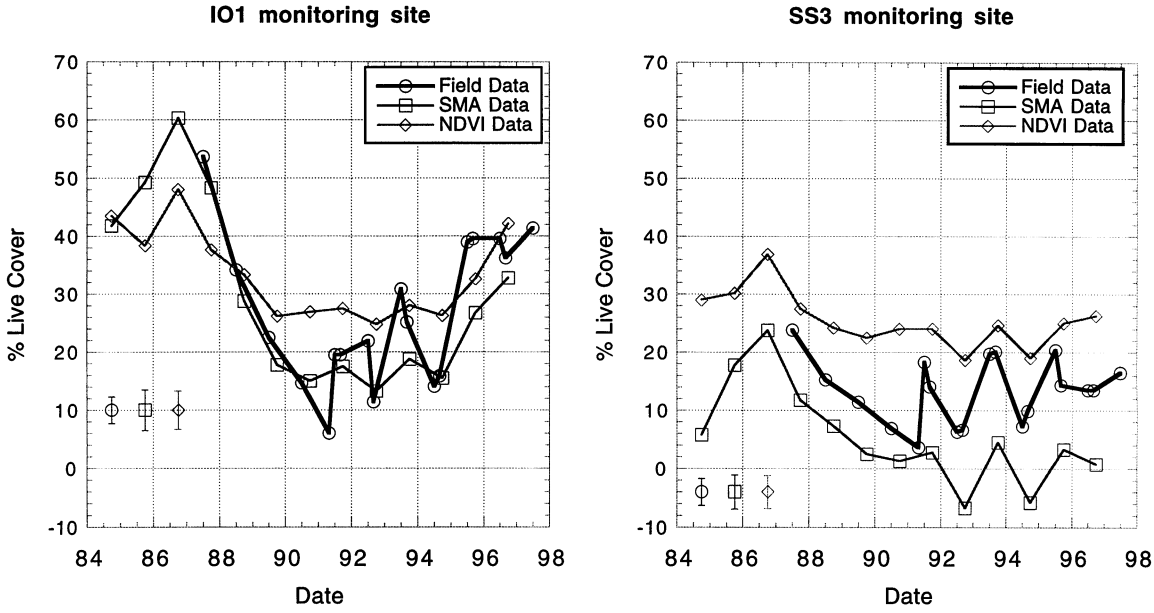

Figure 7. Percent live cover as a function of time as measured in the field compared against SMA and NDVI for two example monitoring sites. (a) Site IO1 shows excellent correlation through time with SMA results. Field measurements were collected more frequently, hence seasonal changes in %LC can be seen while the SMA and NDVI data shows only yearly changes. (b) Site SS3 illustrates an offset between SMA results and the field data. This offset is relatively constant through time and can be attributed to characteristics of the vegetation at the site. Note that NDVI tracks the general shape of change, but is sometimes incorrect in the yearly direction of change. For this plot, standard NDVI values were scaled to be comparable in value to field and SMA measurements.

erty of a single image), we can remove an estimate of this bias and normalize the SMA and NDVI data to a single field measurement. The SMA and NDVI data normalized to the 1991 field data are shown in Fig. 8. This is an additive normalization where the difference between the image and field data in 1991 is subtracted from every subsequent image measurement. As shown in Fig. 8a for the SMA results, this process shifted the data

Figure 8. Percent live cover determined from (a) SMA and (b) NDVI compared to field %LC after removing the bias estimated as the difference between satellite and field values in 1991.

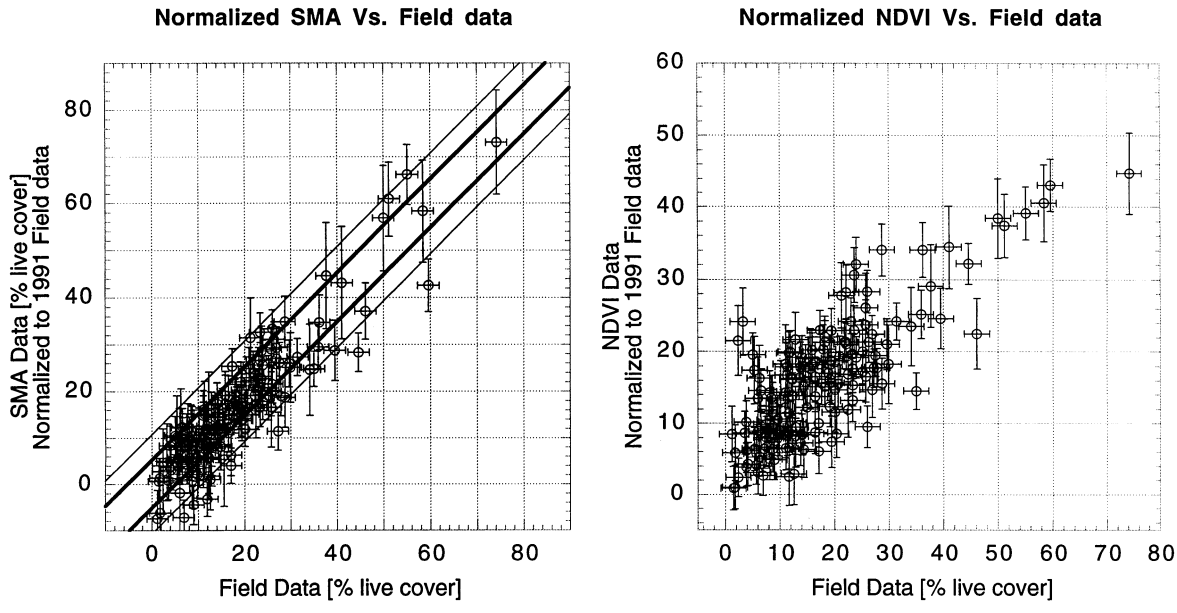

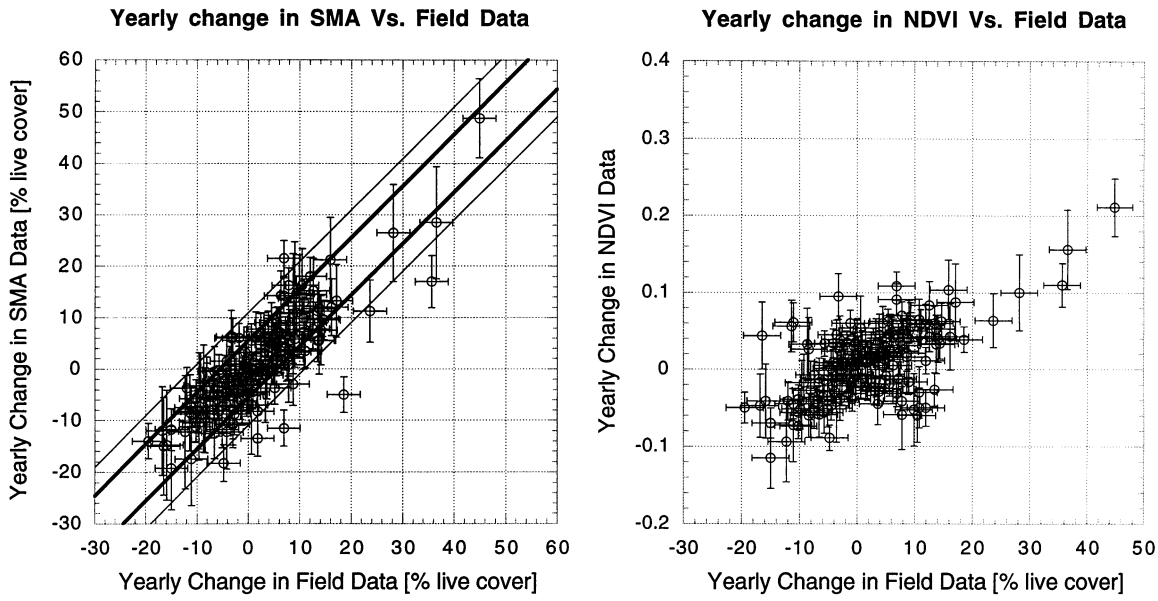

Figure 9. Yearly changes in (a) SMA and (b) NDVI compared against yearly changes in field measures of %LC. For (a) lines at ±3.8 and 7.6%LC are shown about the 1:1 line.

cloud in Fig. 5a to a better fit within the one-to-one line. NDVI does not demonstrate the same improvement with normalization (Fig. 8b) as more scatter is introduced and therefore less of a correlation to the field data is observed.

Measuring Change in Vegetation Cover

Yearly change detection is important for assessing vegetation community health. To assess the correspondence in the annual estimates of vegetation change between the field and remote measurements, we subtracted from each %LC measurement the %LC calculated for the year preceding it. As shown in Fig. 9a, the SMA model produced an excellent estimate of change in %LC: The value of change calculated using SMA nearly equals the value of change measured in the field. These values are plotted in a histogram in Fig. 10 and show that the data cloud is centered on the one-to-one line. The mean distance to this line is 0.70%LC. However, using the standard deviation of 3.8 %LC and an assumed mean value of 0.0 %LC, these data are consistent with a normal distribution (Kolmogorov-Smirnov test of normality). These results showed that SMA accurately measured change in %LC and can be used to effectively monitor changes in semiarid vegetation. The NDVI data plots in a tighter cluster near-zero change than the SMA data (Fig. 9b), thus making it less useful for detecting change. A very poor correlation coefficient of r^2=0.25 was found for the relationship between NDVI and field measures of %LC (Table 3). As documented previously, the sensitivity of NDVI to soil brightness may be contributing to the sensitivity of NDVI to changes in greenness (Huete et al., 1985). These issues will be discussed further in the discussion.

The data distribution in Fig. 10 has roughly the same standard distribution as that in Fig. 6. This indicates that the measurement precision is nearly identical for yearly change measurements as for absolute measurements. However, the absolute measurement data distribution does not have the same accuracy as the yearly change data distribution. This is demonstrated by the fact that the absolute measurements include a bias of about 2.3 %LC from the one-to-one line while the yearly change measurements fall directly over the one-to-one line (Table 3).

DISCUSSION

Quantitative analyses of change with multitemporal remotely sensed data must begin with careful attention to radiometric calibration and coregistration. The radiometric methods used here provided a reliable and consistent approach to achieving radiometric consistency across the 14 years of satellite data. It is preferable to achieve the same result using first principles (i.e., time, date, location of measurement; atmospheric conditions). However, approaches based on first principles have not yet achieved the reliability and consistency of the empirical methods used here.

Smith et al. (1990a) previously made the most robust comparison between SMA and field data. They showed that SMA results correlated with field data with r^2 values between 0.80 and 0.91. They used reference endmembers as opposed to image endmembers; thus the vegetation endmember was a leaf spectra rather than a canopy

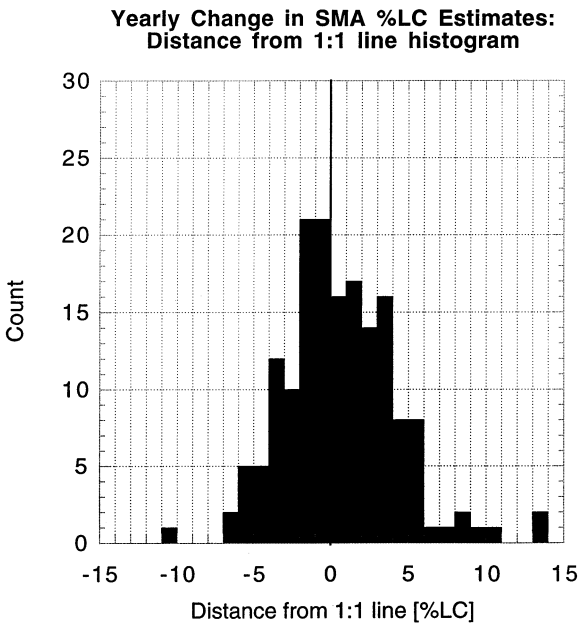

Figure 10. Histogram of the absolute %LC estimates from Fig. 9a show the distribution of the data about the one-to-one line. Note that in this case the peak falls more closely to the one-to-one line than in Fig. 6.

level spectrum. For vegetation, this resulted in an underestimation of field measures of live cover (i.e., a slope other than 1.0). Using these results as a benchmark, we have shown that image endmembers can be used to obtain the same quality of result (our data in Fig. 5a has a similar correlation of 0.88) (Table 3). The most significant difference between the Smith et al. (1990a) data and the data presented here is the slope of the regression line between SMA results and field measures of live cover. Smith et al. (1990a) detected a significant deviation in slope from the one-to-one line, while our results indicate a very close approximation to the one-to-one line. Furthermore, Smith et al. (1990a) found a different slope for field sites containing primarily bajada vegetation versus sites containing phreatophyte vegetation. These two types of vegetation have different community structure and species, which supports our reasoning that the slope depends on the structural properties of the vegetation community. Other work shows that plant structure is the single most important factor influencing canopy level reflectance (Asner, 1998).

The comparison of field and remotely sensed data for the same site over many years further supports the hypothesis that bias between remote and field measures are related to field conditions. When the SMA results are reduced to a measure of annual change in %LC and compared with the same measure in the field data, the bias in the results were removed. However, the variance of the results is largely unchanged (Table 3). Further research may reveal whether the bias observed in using SMA to directly measure %LC was primarily due to endmember selection or if knowledge of vegetation and community structure or soil background could be used in refinements to this approach. Nevertheless, as demonstrated here the change in %LC was accurately and precisely measured with SMA and TM data independent of soil and vegetation community and/or structure variability.

Vegetation endmember selection impacts the correspondence between the SMA results and field measures of %LC. In this work, we chose an endmember from local riparian vegetation; however, all of our field sites are located in shrub and meadow communities. Therefore the small aggregate bias between field and remote measures of %LC might be due to this discrepancy between the endmember canopy structure and that of the average field site. To test this assertion, we chose several alternative vegetation endmembers from the Landsat dataset and completed SMA. In choosing alternative endmembers we were consistent in our constraint of only using areas of high %LC: riparian zones, irrigated crops, and irrigated fields of natural vegetation.

Different vegetation endmembers typically changed the relationship found between SMA results and field measurements of %LC. Use of endmembers from irrigated areas, whether native or nonnative species, tended to underestimate the field measures of live cover to a greater extent. This result is not surprising given the large difference between the reflectance of an irrigated field in the VIS and NIR and that of natural semiarid shrub vegetation. These results also agree with the findings of Smith et al. (1990a), who used a reference leaf spectrum for a vegetation endmember. Spectra taken from irrigated fields always show a much stronger NIR response than natural vegetation. However, multiple endmembers taken from riparian vegetation showed a similar relationship to field measures, regardless of loca-

Table 3. Correlation Results

Measurement Type	*Mean distance to 1:1 line (%LC)*	*Stdev about 1:1 line (%LC)*	*Correlation Coefficient*
SMA: absolute	2.29	3.95	0.88
SMA: normalized	1.39	3.80	0.91
SMA: yearly change	0.70	3.83	0.84
NDVI: absolute	N/A	N/A	0.83
NDVI: normalized	N/A	N/A	0.81
NDVI: yearly change	N/A	N/A	0.25

tion. This type of vegetation, although different in structure and species type, was shown here to reasonably represent 100% cover of semiarid shrub vegetation.

The most significant limitation in using NDVI to quantify change in %LC is the weak relationship between changes in NDVI and changes in %LC. To quantify vegetation abundance, NDVI must first be calibrated to field measures of vegetation. Furthermore, problems with soil-brightness effects on NDVI and other VIs have been shown to interact in a complicated manner. Huete et al. (1985) showed that NDVI varied as much as 0.3 with changes in bare soil NIR reflectance. Additionally, this effect was not consistent across different levels of vegetation %LC. For example, a change in live cover from 40% to 60% over a soil NIR reflectance of 25% will result in an NDVI change of 0.2, while the same change over a dark soil (5% NIR reflectance) results in an NDVI change of only 0.1. Therefore, background soil brightness directly and inconsistently affects the NDVI measurement of changes in %LC. When many different field sites are being used in the analysis, soil brightness can account for much of the scatter observed in relationships like those in Fig. 9b.

Studies that assume changes in NDVI relate linearly with field measures of vegetation change lose precision. We have shown that this point is significant, even when large changes in field vegetation are being considered. Other studies (e.g., Purevdorj et al., 1998) have fit a second-order polynomial to plots of NDVI vs. field vegetation measurements. These fits are significantly better than linear regressions. However, the obvious trade-off is a more complicated relationship that requires more data to constrain properly. In addition, these approaches have not been shown to be robust against multiple soil backgrounds and vegetation communities.

The relationship between SMA and %LC was robust as the analysis proceeded from absolute values through to an assessment of change. In contrast, the relationship between field measurements of %LC and NDVI became weaker. This trend is perhaps best illustrated in Fig. 9. When assessing change in a landscape, it is equally important to get the correct magnitude and sense of change (i.e., positive or negative changes). The SMA results show that this technique indicates the correct sense of change in 86% of the data. For NDVI, however, the correct sense of change is indicated in only 67% of the data.

SUMMARY AND CONCLUSIONS

SMA can be used to make quantitative measurements of change in %LC with a precision better than 4.0 %LC. Absolute measurements of live cover typically included a bias from field measurements though the sense of bias (positive or negative) varied. Part of this bias is expected given that image endmembers were used in the SMA model, but regardless of endmember selection, one cannot use a single endmember to remove all bias. This is an inherent limitation of SMA applied to coarse spectral resolution data. Part of the bias, however, is due to other factors such as local vegetation community and structure. Nevertheless, we have clearly shown that bias between remotely measured and field measured %LC can be simply removed by focusing on the quantification of change. Thus, when the change in %LC is the key parameter to be determined, SMA provides a very precise tool. Due to the robust nature of this method, it is likely that these results could be extended to ecosystem and land cover types different from those studied here. For studies that use this method in ecosystems other than semiarid, SMA is a precise tool in the measurement of changes in %LC. However, absolute measurements of %LC should be validated against field measurements.

NDVI is a simple and reliable measure of greenness in remotely sensed data for a single date. While NDVI values showed a significant correlation to field measures of vegetation, this relationship was less robust when subsequent measurements were subtracted from each other to measure change. As discussed, we suspect that this effect is largely due to the documented soil brightness effects on NDVI (Huete et al., 1985). Qualitatively, NDVI will generally show the proper sense of change in greenness. However, the SMA results indicated the correct sense of change in a larger number of our samples and gave precise estimates of the magnitude of that change.

Vegetation communities in semiarid and arid regions are principally limited in their productivity by the availability of water. Thus significant changes in water availability will be reflected in the growth and decline of these communities. The ability to precisely determine percent live cover with remotely sensed data will have important applications to a range of problems in these regions including climate change and response to anthropogenic modifications. The results of this study establish critical limits on the precision and accuracy of vegetation abundance determined from Landsat TM data using SMA. Future work will now focus on understanding the causes of observed changes.

We would like to thank Thompson Webb III, Steven Hamburg, and Aaron Steinwand for helpful comments while preparing this manuscript; the Inyo County Water Department and the Los Angeles Department of Water and Power for providing expertise and important data; and an anonymous reviewer for excellent comments on the manuscript. Support from NASA's Land Use/Land Cover Change program (Grant # NAG5-6003) is gratefully acknowledged.

REFERENCES

Adams, J. B., and Adams, J. D. (1984), Geologic mapping using Landsat MSS and TM images: Removing vegetation by modeling spectral mixtures. In *Third Thematic Conference on Remote Sensing for Exploration Geology*, Colorado Springs, CO, USA, ERIM 2, pp. 615–622.

Adams, J. B., Sabol, D., Kapos, V., Almeida Filho, R., Roberts, D. A., Smith, M. O., and Gillespie, A. R. (1995), Classification of multispectral images based on fractions of endmembers: Application to land-cover change in the Brazilian Amazon. *Remote Sens. Environ.* 52:137–154.

Adams, J. B., Smith, M. O., and Gillispie, A. R. (1993), Imaging spectroscopy: Interpretations based on spectral mixture analysis. In *Remote Geochemical Analysis: Elemental and Mineralogical Composition* (C. M. Pieters and P. A. Englert, Eds.), Cambridge University Press, Cambridge, UK, pp. 145–166.

Adams, J. B., Smith, M. O., and Johnson, P. E. (1986), Spectral mixture modeling: A new analysis of rock and soil types at the Viking Lander 1 site. *J. Geophys. Res.* 91:8098–8112.

Asner, G. P. (1998), Biophysical and biochemical sources of variability in canopy reflectance. *Remote Sens. Environ.* 64:234–253.

Borel, C. G., and Gerstl, S. A. W. (1994), Nonlinear spectral mixing models for vegetative and soil surfaces. *Remote Sens. Environ.* 47:403–416.

Davis, J. C. (1986), *Statistics and Data Analysis in Geology*, John Wiley and Sons, New York, pp. 99–103.

Duncan, J., Stow, D., Franklin, J., and Hope, A. (1993), Assessing the relationship between spectral vegetation indices and shrub cover in the Jornada Basin, New Mexico. *Int. J. Remote Sens.* 14:3395–3416.

Elvidge, C. D., and Lyon, R. J. P. (1985), Influence of rock-soil variation on the assessment of green biomass. *Remote Sens. Environ.* 17:265–279.

Garcia-Haro, F. J., Gilabert, M. A., and Melia, J. (1996), Linear spectral mixture modeling to estimate vegetation amount from optical spectral data. *Int. J. Remote Sens.* 17:3373–3400.

Gillespie, A. R., Smith, M. O., Adams, J. B., Willis, S. C., Fischer, A. F. III, and Sabol, D. E. (1990), Interpretation of residual images: Spectral mixture analysis of AVIRIS images, Owens Valley, California. In *Proceedings of the Second Airborne Visible/Infrared Imaging Spectrometer (AVIRIS) Workshop* (R. O. Green, Ed.), JPL publication 90-54, pp. 243–270.

Graetz, R. D., and Gentle, M. R. (1982), The relationship between reflectance in the Landsat wavebands and the composition of an Australian semi-arid shrub rangeland. *Photogramm. Eng. Remote Sens.* 48(11):1721–1730.

Hall, F. G., Strebel, D. E., Nickeson, J. E., and Goetz, S. J. (1991), Radiometric rectification-toward a common radiometric response among multidate, multisensor images. *Remote Sens. Environ.* 35:11–27.

Hickman, J. C. (1993), *The Jepson Manual: Higher Plants of California*, University of California, Berkeley.

Holland, R. F. (1986), *Preliminary Descriptions of the Terrestrial Natural Communities of California.* Unpublished report of California Department of Fish and Game, Natural Diversity Data Base, Sacramento, CA.

Hollett, K. J., Danskin, W. R., McCaffrey, W. F., and Walti, C. L. (1991), *Geology and Water Resources of Owens Valley, California.* U.S. Geological Survey Water Supply Paper 2370.

Horowitz, H. M., Lewis, J. T., and Pentland, A. P. (1975), *Estimating Proportion of Objects from Multispectral Scanner Data.* Final Report, NASA-CR-141862, pp. 108.

Huete, A. R. (1988), A soil adjusted vegetation index (SAVI). *Remote Sens. Environ.* 25:295–309.

Huete, A. R., and Tucker, C. (1991), Investigation of soil influences in AVHRR red and near-infrared vegetation index imagery. *Int. J. of Remote Sens.* 12:1223–1242.

Huete, A. R., Jackson, R. D and Post, D. F. (1985), Spectral response of a plant canopy with different soil backgrounds. *Remote Sens. Environ.* 17:37–53.

Inyo County and City of Los Angeles (1990), Technical Appendix F: Green book for the long-term groundwater management plan for the Owens Valley and Inyo County. In: *Draft Environmental Impact Report: Water from the Owens Valley to Supply the Second Los Angeles Aqueduct; 1970 to 1990, and 1990 Onward, Pursuant to a Long Term Groundwater Management Plan.* Los Angeles Department of Water and Power and County of Inyo, Los Angeles, CA. SCH #89080705.

Jackson, R. D. (1983), Spectral indices in N-space. *Remote Sens. Environ.* 14:409–421.

Johnson, P. E., Smith, M. O., Taylor-George, S., and Adams, J. B. (1983), A semiempirical method for analysis of the reflectance spectra of binary mineral mixtures. *J. Geophys. Res.* 88:3557–3561.

Kuchler, A. W. (1988), The map of the natural vegetation of California. In *Terrestrial vegetation of California* (M. G. Barbour and J. Major, Eds.), California Native Plant Society, Special Publication Number 9, pp. 909–938.

Lyon, J. G., Yuan, D., Lunetta, R. S., and Elvidge, C. D. (1998), A change detection experiment using vegetation indices. *Photogramm. Eng. Remote Sens.* 64:143–150.

MacMahon, J. A. (1988), Warm deserts. In *North American Terrestrial Vegetation* (M. G. Barbour and W. D. Billings, Eds.), Cambridge, New York, pp. 232–264.

Major, D. J., Baret, F., and Guyot, G. (1990), A ratio vegetation index adjusted for soil brightness. *Int. J. Remote Sens.* 11:727–740.

Mustard, J. F., and Pieters, C. M. (1987), Abundance and distribution of ultramafic microbreccia in Moses rock dike: Quantitative application of mapping spectrometer data. *J. Geophys. Res.* 92:13619–13634.

Mustard, J. F., and Pieters, C. M. (1989), Photometric phase functions of common geologic minerals and applications to quantitative analysis of mineral mixture reflectance spectra. *J. Geophys. Res.* 94:13619–13634.

Pech, R. P., Graetz, R. D., and Davis, A. W. (1986), Reflectance modeling and the derivation of vegetation indices for an Australian semi-arid shrubland. *Int. J. Remote Sens.* 7(3):389–403.

Purevdorj, T. S., Tateishi, R., Ishiyama, T., and Honda, Y. (1998), Relationships between percent vegetation cover and vegetation indices. *Int. J. Remote Sens.* 19:3519–3535.

Ray, T. W., and Murray, B. C. (1996), Nonlinear spectral mixing in desert vegetation. *Remote Sens. Environ.* 55:59–64.

Roberts, D. A., Adams, J. B., and Smith, M. O. (1993), Discriminating green vegetation, non-photosynthetic vegetation and soils in AVIRIS data. *Remote Sens. Environ.* 44(2/3):255–270.

Roberts, D. A., Green, R. O., and Adams, J. B. (1997), Temporal and spatial patterns in vegetation and atmospheric properties from AVIRIS. *Remote Sens. Environ.* 62:223–240.

Rouse, J. W., Haas, R. H., Schell, J. A., and Deering, D. W.

(1973), Monitoring vegetation systems in the Great Plains with ERTS. In *Third ERTS Symposium*, Vol. I**<<?6>>**.

Schott, J., Salvaggio, C., and Volchok, W. (1988), Radiometric scene normalization using pseudoinvariant features. *Remote Sens. Environ.* 26:1–16.

Singer, R. B., and McCord, T. B. (1979), Mars: Large scale mixing of bright and dark surface materials and implications for analysis of spectral reflectance. In *Proceeding of the Lunar Planetary Science Con. 10th*, Houston, TX, USA, pp. 1835–1848.

Smith, M. O., Ustin, S. L., Adams, J. B., and Gillespie, A. R. (1990a), Vegetation in deserts: I. A regional measure of abundance from multispectral images. *Remote Sens. Environ.* 31:1–26.

Smith, M. O., Ustin, S. L., Adams, J. B., and Gillespie, A. R. (1990b), Vegetation in deserts: II. Environmental influences on regional abundance. *Remote Sens. Environ.* 31:27–52.

Sohn, Y., and McCoy, R. M. (1997), Mapping desert shrub rangeland using spectral unmixing and modeling spectral mixtures with TM data. *Photogramm. Eng. Remote Sens.* 63:707–716.

Sorenson, S. K., Dileanis, P. D., and Branson, F. A. (1991), *Soil and vegetation Responses to Precipitation and Changes in Depth to Ground Water in Owens Valley.* California: U.S. Geological Survey Paper 2370, Chapter G, Washington, D.C., United States Government Printing Office.

Todd, S. W., and Hoffer, R. M. (1998), Responses to spectral indices to variations in vegetation cover and soil background. *Photogramm. Eng. Remote Sens.* 64:915–921.

Townshend, J. R. G. (1992), The impact of misregistration on change detection. *IEEE Trans. Geosci. Remote Sens.* 30(5):1054–1060.

Tueller, P. T. (1987), Remote sensing science applications in arid environments. *Remote Sens. Environ.* 23:143–154.

Woodwell, G. M., Hobbie, J. E., Houghton, R. A., Melillo, J. M., Moore, B., Park, A. B., Peterson, B. J., and Saver, G. R. (1984), Measurement of changes in the vegetation of the earth by satellite imagery. In *The Role of Terrestrial Vegetation in the Global Carbon Cycle: Measurement by Remote Sensing*, SCOPE 23 (Woodwell, G. M., Ed.), Wiley, New York, pp. 221–240.